JACS
JOURNAL OF THE AMERICAN CHEMICAL SOCIETY
Article
pubs.acs.org/JACS

Heterogeneous Nucleation of Ice on Carbon Surfaces

Laura Lupi, Arpa Hudait, and Valeria Molinero*

Department of Chemistry, The University of Utah, 315 South 1400 East, Salt Lake City, Utah 84112-0850, United States

ABSTRACT: Atmospheric aerosols can promote the heterogeneous nucleation of ice, impacting the radiative properties of clouds and Earth's climate. The experimental investigation of heterogeneous freezing of water droplets by carbonaceous particles reveals widespread ice freezing temperatures. It is not known which structural and chemical characteristics of soot account for the variability in ice nucleation efficiency. Here we use molecular dynamics simulations to investigate the nucleation of ice from liquid water in contact with graphitic surfaces. We find that atomically flat carbon surfaces promote heterogeneous nucleation of ice, while molecularly rough surfaces with the same hydrophobicity do not. Graphitic surfaces and other surfaces that promote ice nucleation induce layering in the interfacial water, suggesting that the order imposed by the surface on liquid water may play an important role in the heterogeneous nucleation mechanism. We investigate a large set of graphitic surfaces of various dimensions and radii of curvature and find that variations in nanostructures alone could account for the spread in the freezing temperatures of ice on soot in experiments. We conclude that a characterization of the nanostructure of soot is needed to predict its ice nucleation efficiency.

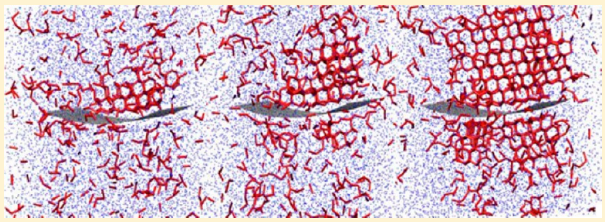

INTRODUCTION

The radiative properties of clouds are strongly influenced by the formation of ice particles.[1] Heterogeneous nucleation of ice on aerosols of various origins is the main mechanism of formation of ice in the atmosphere.[1−5] On a molecular level, ice nucleation by a surface remains poorly understood. A growing body of experimental studies of heterogeneous nucleation of ice shows a wide range of ice nucleation ability among atmospheric particles.[2,3,5−32] The microscopic mechanisms underlying heterogeneous ice freezing and the characteristics that make some surfaces more effective for ice nucleation are not yet known.[2,3] It has been long assumed that good ice nucleating surfaces have the ability to make strong bonds with water and induce ice-like order through specific chemical interactions, effectively templating the formation of ice.[33,34] New results, however, demonstrate that these requirements are not always met.[2,35]

Carbon surfaces are a primary source of atmospheric aerosols.[36,37] Carbonaceous particles are emitted to the atmosphere during combustion processes and account for 10% of the tropospheric particulate matter.[36] Emissions are estimated to be in the range of 12−24 Tg yr^{-1}.[2,36,38] Soot, the fine particulate material produced by combustion, is composed mostly by graphitic layers. Soot displays a great variability of ice nucleation ability:[18−29] freezing temperatures ranging from −18 and −34 °C have been reported.[2,18,20] The origin of the great dispersion of efficiencies among carbonaceous compounds is not understood. Some reports indicate that oxidative aging occurring in the atmosphere improves the ice nucleation efficiency of soot.[39−43] Oxidation also results in an increase of curvature of graphitic lamellae,[44−47] altering the nanostructure of soot.

The chemical functionalization and nanostructure of carbon surfaces can impact their ability to nucleate ice. Unoxidized graphitic surfaces interact weakly with water and cannot directly template the formation of ice. Soot can have a variable composition of epoxy, carbonyl, hydroxyl, and carboxylate groups (among others) depending on its origin and processing conditions.[48,49] Reports indicate that oxidation occurs preferentially at the edge of the graphitic lamellae.[45,50] Recent studies conclude that the distribution of hydroxyl groups on graphite oxide is not random.[51,52] The actual spatial distribution of functional groups in soot is not known, but there is no evidence that they are organized in patterns that match (i.e., template) the crystalline structure of ice.

Soot particles present great variability in nanostructure.[22,49,53−55] The goal of this work is to investigate the effect of variations in the nanostructure of graphitic lamellae on the freezing temperatures of ice. In separate work, we address the effect of hydroxylation and hydrophilicity of graphitic surfaces on the nucleation of ice.[56] Nanoscopic structural characteristics of soot are controlled by three factors: source fuel, temperature, and flow rate.[54] Soot generated at low temperature from different fuel sources exclusively has amorphous structure, at higher temperature lower flow rate generates flat graphitic surfaces, while higher flow rate generates curved surfaces.[54] The radius of curvature of graphitic lamellae in soot ranges from 2 to 50 nm,[22] and the typical lamella dimensions range from 0.5 to 6 nm.[53] The effect of changes in soot nanostructure on ice freezing temperatures has not been previously addressed in the literature.

Received: November 11, 2013
Published: February 4, 2014

   dx.doi.org/10.1021/ja411507a | J. Am. Chem. Soc. 2014, 136, 3156−3164

Existing experimental methods are optimum to determine crystallization rates and freezing temperatures. Nucleation, however, is a rare event involving the stochastic creation of an ice nucleus of nanoscopic dimensions within the liquid. State of the art experimental techniques do not have the spatial and temporal resolution to investigate the microscopic process of nucleation. Molecular simulations have the appropriate resolution to investigate the molecular mechanisms that give birth to the ice nuclei and its growth into a crystallite, and have been successfully used to investigate the mechanism of homogeneous nucleation of ice.[57−67] Molecular dynamics,[68,69] Monte Carlo simulations,[70−75] and density functional theory[76,77] have been used to study the structural modification imposed on water by the presence of particles that are potential ice nucleators, but only a few[35,78−80] simulation studies focused on nucleation of ice from liquid water in the presence of these surfaces. Heterogeneous nucleation of ice has been investigated in the presence of strong electric fields,[78−80] for water confined on nanotubes and in nanoslits[81−83] and on kaolinite.[35]

In this work we use molecular dynamics simulations to investigate the heterogeneous nucleation of ice in the presence of model surfaces that correspond to the main building blocks of soot: graphitic surfaces with the range of lamellae sizes and radii of curvature observed in the experiments. The study of crystallization of water through molecular simulations is challenging because it requires very long simulations or the use of simulation techniques to sample rare events. To overcome this difficulty, in this work we use the coarse grained model of water mW.[84] Simulations with mW water are over 2 orders of magnitude computationally more efficient than atomistic simulations, allowing for simulation cells much larger than the critical ice nuclei and thus for results that are not affected by finite size effects. The mW water model reproduces the anomalies and structures of liquid water, ices, and amorphous solid water and the transitions between them.[58,59,61,63−65,83−93] mW has been successfully used to investigate the homogeneous nucleation of ice from bulk water,[58,59,61,88,92,93] solutions,[63] nanodroplets,[64,66] and in nanopores.[65]

To our knowledge, the present study is the first to compute heterogeneous freezing temperatures for ice on *any* surface through molecular simulations. We provide an analysis of the ice nucleation efficiency of a surface as measured by the gap between the temperatures of homogeneous and heterogeneous freezing, as it is usually reported in experiments. The results of this work indicate that variations in lamella size and curvature within the ranges reported in the nanostructural characterization of soots could account for the observed dispersion in ice freezing temperatures. Controlled experiments with particles of well-characterized nanostructure would provide insights on the identification of the characteristics of surfaces that are the most relevant for the heterogeneous nucleation of ice.

METHODS

Systems. We investigated the nucleation of ice on atomically flat planar and curved graphitic surfaces and compared the results with a rough surface of comparable hydrophobicity. The graphitic surfaces were built with VMD.[94] Graphite was modeled as a single layer of graphene with water−carbon interactions that reproduce the experimental contact angle for water on graphite. The graphite layer was periodic in the plane of the surface. Periodic surfaces with dimensions 5 × 5 nm^2 were embedded in bulk water (modeled with 4,096 or 10,000 water molecules) or in contact with slabs of water (4,096 molecules). Water droplets (5,241 molecules) were studied over periodic 8 × 8 nm^2 graphitic surfaces. Graphitic lamellae consisted of disks cut from the graphite layer, with diameters ranging from 1.5 to 4 nm. Simulation cells containing a single of these lamellae immersed in 4,096 water molecules were used for the crystallization simulations. Curved graphitic surfaces with radii of curvature 27.1, 6.8, and 2 nm were built by cutting 5 × 5 nm pieces from single-walled carbon nanotubes with the corresponding radii of curvature. These curved surfaces were embedded in simulation cells containing 10,000 water molecules. A rough hydrophobic surface was prepared by immobilizing a slab of water molecules of a bulk simulation of liquid water at 298 K following the procedures of ref 86. The width of the interface of the rough surfaces, as measured by the t_{90-10}, is 1.4 Å, half the width of a water molecule.[65] The surface has a contact angle equivalent to that of water on graphite.[86]

Force Fields. The interaction between water molecules is described by the monatomic water model mW.[84] The mW model of water does not have hydrogen atoms or electrostatics and represents each water molecule as a single particle able to form tetrahedral "hydrogen-bonded" structures through three-body nonbonded interactions. The interactions between mW water molecules consist of a sum of pairwise and three-body contributions described by the functional form of the Stillinger−Weber (SW) potential.[95] The interaction between water and carbon in the graphitic surfaces is described by a two-body SW potential, where the size and strength of the water−carbon interaction parameters have been tuned in order to obtain the experimental contact angle for graphite, 86°:[96,97] σ_{WC} = 0.32 nm, ε_{WC} = 0.13 kcal/mol. The contact angle was determined following the procedures of ref 86. The interaction of water with the rough hydrophobic surface is also represented by a two-body SW potential characterized by σ_{WC} = 0.32 nm, ε_{WC} = 0.3 kcal/mol.[86] The equations of motion of the atoms of the graphitic surfaces are not integrated (i.e., they are fixed); therefore, there is no need to define carbon−carbon interaction potentials.

Simulation Settings. Molecular dynamics simulations were evolved using LAMMPS.[98] The equations of motion of water were integrated with the velocity Verlet algorithm with a time step 5 fs in the case of the systems with an open water/vacuum interface and 10 fs for the bulk systems. The simulation cells with droplets or slabs were treated with periodic boundary conditions in the dimensions corresponding to the surface plane; the bulk systems were periodic in the three dimensions. Simulations were performed in the *NVT* ensemble in the case of the water nanodroplets and water slabs and in the *NPT* ensemble for the systems without water/vacuum interfaces. The crystallization of water was investigated through cooling ramps and isothermal simulations. The ramps were performed with cooling rates of 5, 2, and 1 K/ns. Only the latter resulted in crystallization of ice. Isothermal simulations were carried out at temperatures ranging from 210 to 300 K. The temperature and pressure in the simulations were controlled with Nose−Hoover thermostat and barostat with relaxation times 0.5 and 2.5 ps, respectively. To determine error bars in the freezing temperatures, we performed 5 repetitions of each quenching simulation for every system, for a total of 65 cooling simulations and 29 isothermal simulations.

Analysis. *Ice* was identified with the order parameter q_6 computed for the individual water molecules along the simulation trajectories.[99] A cutoff value of 0.58 was found to provide a clear distinction between ice and supercooled liquid water. The *largest ice cluster* was identified by clustering the water molecules with $q_6 > 0.58$ using a cutoff distance of 0.35 nm. The *size of the critical nuclei* was estimated from the analysis of isothermal crystallization runs as the size of the largest ice cluster, N_{ice}, before the cluster grows irreversibly leading to the crystallization of the whole system. The *ice crystallization (or freezing) temperature*, T_f, was determined as the onset of increase in the fraction of ice when each system is cooled at a rate of 1 K/ns, the fastest cooling rate that results in ice formation for mW water.[59] We found that faster cooling rates, at 2 or 5 K/ns, did not result in ice crystallization with any of the surfaces of this study. We quantified the *layering of water at the surface* calculating the density distributions of mW molecules along the direction normal to the surface. In the case of the droplets the layering has been computed only for the water

dx.doi.org/10.1021/ja411507a | J. Am. Chem. Soc. 2014, 136, 3156−3164

molecules in a cubic box inscribed in the droplet to avoid surface effects. Layering was determined from isothermal simulations, for which we equilibrated at least 5 ns before the production runs.

RESULTS AND DISCUSSION

A. Graphite Promotes the Heterogeneous Nucleation of Ice. We first determined the nonequilibrium freezing temperature T_f of water in contact with flat, "infinite" graphite surfaces. Crystallization is a stochastic process; therefore, we performed five independent evaluations of T_f on each of the four flat graphite surfaces. The periodic graphite surfaces promoted heterogeneous nucleation of ice in all simulations. The temperature of homogeneous ice nucleation for the mW water model is $T_f^{homo} = 201 \pm 1$ K.[59] We report our results in terms of the freezing efficiency of the surface, the increase of freezing temperature with respect to the homogeneous freezing temperature, $\Delta T_f = T_f - T_f^{homo}$, to facilitate the comparison with experiments. The freezing efficiency ΔT_f for ice on graphite for the four systems we studied were indistinguishable within their error bars: 11 ± 1 K for the droplets, 13 ± 3 K for slabs, 11 ± 2 K for bulk with 4096 water molecules, and 13 ± 2 K for bulk with 10,000 water molecules. On average, the simulations predict that the crystallization temperature of ice on the graphite surface is 12 ± 3 K higher than the temperature of homogeneous ice nucleation. These results are in excellent agreement with experimental data, which indicates that ice freezing temperatures on carbon surfaces occur at a maximum of 16 K above the homogeneous crystallization limit.[18,20] The ice that resulted from nucleation on graphite was a hybrid ice I with short stacks of hexagonal and cubic layers[92,100−102] oriented with the stacking faults parallel to the graphitic surface, in agreement with the experimental structure of ice obtained by vapor deposition on carbon surfaces.[103]

Figure 1 presents snapshots along a typical crystallization trajectory of a water droplet on graphite at 6 K above the freezing temperature of mW water on this surface. Three significant results can be gleaned from this figure.

i) Subcritical ice nuclei, containing less than 100 water molecules, formed through all the droplet volume (panel A and B of Figure 1) during the induction period. *Critical nuclei, however, formed only at the graphite surface* (panel C). We do not find evidence for preferential ice nucleation at the water/vapor interface. The critical nuclei contained between 100 and 200 water molecules, the same as for homogeneous nucleation of water at the homogeneous nucleation temperature.[59,104]

ii) *There is not a premelted or disordered water layer between ice and the graphite surface.* "Wetting" of the surface by ice is consistent with a stabilization of the ice nuclei by the surface, a precondition for heterogeneous nucleation. It should be noted, however, that we do not observe layer-by-layer growth of ice from the surface in any of the simulations: the nucleation of ice on the graphite surfaces is not barrierless. According to classical nucleation theory a favorable contact angle between the ice embryos and the surface can account for a favorable free energy of nucleation. The contact angle between a crystal and a solid surface, however, is not a well-defined property.

iii) *Liquid water layers at the graphitic surface.* The density profile of water in the direction perpendicular to the surface presents sharp oscillations, which are the most pronounced at the distances corresponding to the first and second layer ice in contact with the surface (Figure 2). Water layering has been previously reported for water at 298 K in contact with graphene plates using ab initio[97,105] and atomistic[106] simulations. All

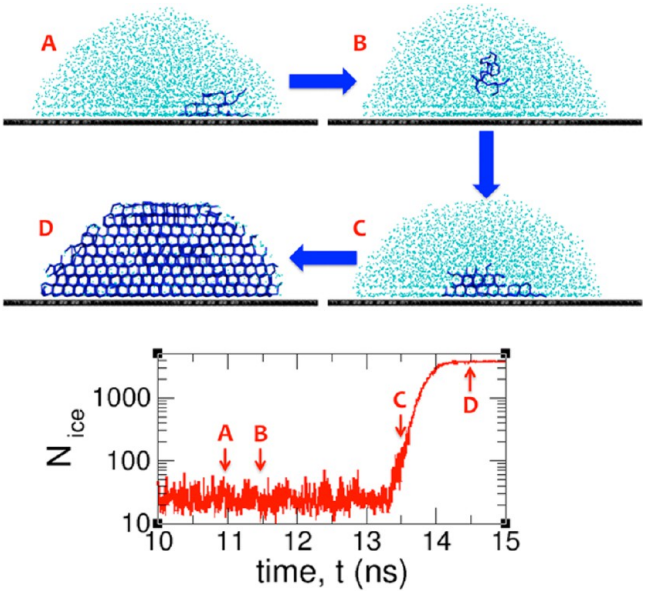

Figure 1. Isothermal crystallization of a water droplet on graphite at T_f + 6 K. Panels A to D show snapshots of the water droplet, which contains ∼5500 water molecules, on the periodic graphite surface, evolved at 218 K. Liquid water is shown with cyan dots, ice crystallites with blue balls and sticks. Snapshots A and B show subcritical ice nuclei at the surface and in the bulk of the droplet, respectively. Snapshot C shows the successful nucleation event at the surface with the formation of the critical nucleus composed of ∼150 water molecules. Snapshot *D* shows the fully crystallized droplet. The lower panel shows the size of ice nucleus (number of water molecules in the largest ice cluster, N_{ice}) as a function of the simulation time, points A-B-C-D correspond to the snapshots of the upper panels.

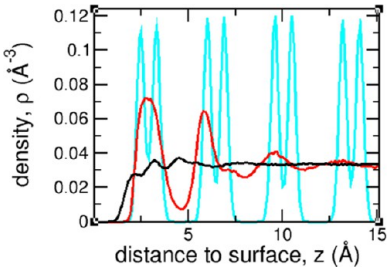

Figure 2. Layering of liquid water at the surfaces. Density profiles of liquid water at 230 K on top of graphite (red line) and the atomically rough hydrophobic slab (black line) and of ice on graphite after crystallization (cyan line); the splitting of the peaks in ice is due to the existence of nonplanar chair conformations in ice I.

features here described for a droplet of water on graphite are confirmed by detailed analysis of the simulation trajectories of slabs and bulk water in contact with the flat periodic carbon surfaces.

An increase in roughness of the surface has been hypothesized to play a role in the decrease of ice nucleation ability of self-assembled monolayers of mixtures of aliphatic alcohols with different chain lengths.[34] To investigate whether the roughness of the surface plays a role on the layering of liquid water and on promoting heterogeneous nucleation of ice, we performed cooling simulations for water in contact with an atomically rough surface with hydrophobicity equivalent to that of graphite. We find that the rough surface does not induce layering of the liquid (Figure 2) and does not promote heterogeneous nucleation of ice: crystallization in the 5

dx.doi.org/10.1021/ja411507a | J. Am. Chem. Soc. 2014, 136, 3156−3164

realizations for the rough hydrophobic surface occurs at T_f^{homo}. The same is observed for hydrophilic rough surfaces,[56] indicating that it is the roughness and not the hydrophobicity of the surface that hinders the heterogeneous nucleation of ice.

Interestingly, simulations indicate that other good ice nuclei, kaolinite[35] and AgI,[70] also induce layering of liquid water at the surface. A recent atomistic simulation study reported ice nucleation in the presence of kaolinite[35] and observed that layering of water seems to be associated with the formation of the ice nucleus. The expense of atomistic simulations limited that study to small systems (192 and 768 water molecules), and the authors noted that the simulations were affected by finite size effects (crystallization was observed for the smaller system but not the larger one, although a larger amount of water should increase the nucleation probability).[35] In the present study, the size of the critical nucleus is much smaller than the number of water molecules in the simulation cells. There are no finite size effects and we find − as Cox et al. in their study with kaolinite[35]− that the surface that induces layering of water heterogeneously nucleates ice. The surface that does not induce layering is unable to promote ice nucleation.

We quantify the degree of order induced by the surfaces on water by the layering L which measures the deviation of the local water density at distance z from the surface, $\rho(z)$, from the average bulk density, ρ^{bulk}, of water, integrated over all the density profile

$$L = \int \left| \frac{\rho(z)}{\rho^{bulk}} - 1 \right|^2 dz \quad (1)$$

where the integral spans from the surface ($z = 0$) to a distance for which the density reaches the bulk average ($z = 1.5$ nm in the present simulations). Previous studies show that layering of water on graphite is evident already at room temperature.[97,105,106] We find that the layering of the liquid increases significantly with undercooling (Figure 3). Layering L of deeply

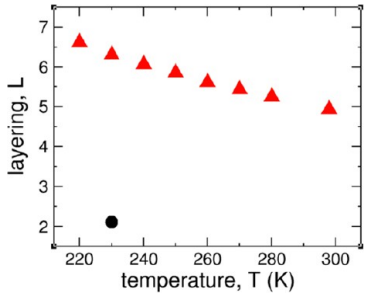

Figure 3. Layering of liquid water increases with supercooling. Layering L of water in contact with graphite (red triangles) and an atomically rough hydrophobic surface (black circle) as a function of temperature. T_f^{homo} is 201 ± 1 K and T_f on graphite is 213 ± 3 K for mW water.[59] Layering on graphite at room temperature is already well above the value of layering at the rough surface at 230 K.

supercooled liquid water on the rough surface that does not induce heterogeneous nucleation, however, is well below, about half, the value for graphite at 298 K. Our results for graphite, together with those for kaolinite[35] and for silver iodide,[70] suggest that the layering already present in interfacial supercooled liquid water facilitates the crystallization of ice at the surface. Different from graphite, kaolinite is hydrophilic and strongly binds to water through its hydroxyl-terminated face. While layering of liquid water on kaolinite may be associated with the water/surface hydrogen-bonding interactions, layering of water on graphite is induced by the flatness of the surface. Silver iodide is, as graphite, a prevalently hydrophobic surface.[107] However, it is not clear whether the ability of AgI to nucleate ice can be attributed to crystallographic matching between this crystal and ice.[32,107,108]

Aliphatic alcohols monolayers can be effective ice nucleating surfaces.[13,34,109] The ability of alcohol monolayers to nucleate ice has been attributed to the matching of the surface areas per alcohol with those per water in ice, modulated by the tilt of the chains and the orientation of the hydroxyl groups at the surface.[34,109] The proposed mechanism for nucleation of ice on the alcohol monalayers is based on templating of the ice structure by the underlying surface. Nucleation of ice on graphite, on the other hand, is not templated by any underlying structure on the surface. Whether layering of liquid water is a prerequisite for heterogeneous nucleation of ice on *any* surface and how does layering of the liquid affect the free energy of formation of the critical ice embryo are important questions that deserve further study.

The increase in layering of liquid water on graphite upon cooling is accompanied by an increase in the local ordering of the first water layer in contact with the surface. Figure 4 shows

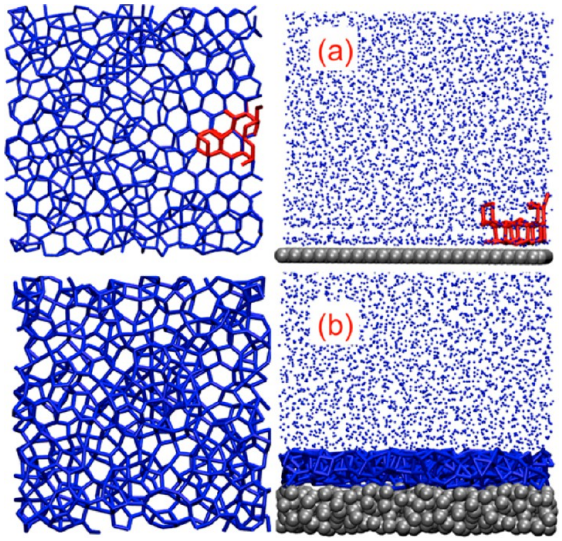

Figure 4. Structure of interfacial water in contact with graphite and with a molecularly rough surface. Snapshots of the simulation box at 220 K for (a) graphite and (b) a molecularly rough surface. Right panels show a lateral view of the simulation boxes and left panels the corresponding front views. In the front views only the first two layers of interfacial water molecules (defined as those within 0.8 nm of the surface, see Figure 2) are shown. Surfaces are shown with gray balls, liquid water with blue dots, the largest ice cluster with red sticks. In the left panels liquid water is shown with blue sticks to highlight bilayer hexagonal patches.

snapshots of water in contact with graphite and the rough surface at 220 K. Panel A captures the critical ice nucleus at the graphite surface. The small crystalline nucleus is surrounded by a patch of bilayer hexagons, which have a crystalline order parameter q_6 close to 0.5, lower than the $q_6 > 0.58$ that characterizes ice. Transient patches of bilayer hexagons appear and disappear at the surface during the induction period that precedes the formation of the critical ice nucleus. We conjecture that the formation of these semiordered structures may play a role in the mechanism of heterogeneous ice

dx.doi.org/10.1021/ja411507a | J. Am. Chem. Soc. 2014, 136, 3156−3164

nucleation on carbon. Two-steps nucleation scenarios, in which thermal fluctuations promote the formation of crystals precursors, i.e. semiordered regions which facilitate the nucleation process, have been proposed for homogeneous nucleation in systems as disparate as ice,[59,60,63,110] clathrate hydrates,[111−113] colloids,[114] calcium carbonate,[115] proteins,[116,117] and hard spheres.[110,118,119] Formation of transient domains of four-coordinated, low-density liquid water precedes the homogeneous crystallization of water.[59,60,63] It is an open question whether the patches of bilayer hexagons play a similar role for the heterogeneous nucleation of ice at graphite surfaces.

B. Variability in Size of Lamellae and Radius of Curvature Could Account for the Spread in Ice Freezing Temperatures on Carbon Particles. Soot from different sources display a wide range of ice freezing temperatures, with freezing efficiency ΔT_f ranging from 0 to 16 K.[2] We have shown in the previous section that the flat graphite surface promotes the heterogeneous nucleation of ice with $\Delta T_f = 12 \pm 3$, in excellent agreement with the largest gap between heterogeneous and homogeneous nucleation temperatures in experiments. It is known that the nanostructure of soot − the radius of curvature of the graphitic particles and the size of the lamellae that conform them − displays a strong variability depending on the soot origin.[54,120] In this section we study the freezing of water in the presence of model graphitic lamellae of different sizes and curvatures in order to understand how does the nanostructure of soot modulate the temperature of crystallization of water.

The size of lamellae in soot varies between 0.5 to 6 nm.[53] For example, diesel soot has a significant percentage of lamellaw larger than 2 nm in length with a comparatively small population in the range of 0.5−1.0 nm, wildfire soot has a very narrow distribution peaked at lamella length below 1 nm, and jet soot has an intermediate distribution that extends from 0.5 to 3 nm.[53] To encompass the range of lamella sizes observed in soot, we studied the crystallization of water in the presence of flat graphitic disks of diameters between 1.5 and 4 nm and compared it with the 5 × 5 nm^2 periodic surface of section A. Figure 5 shows that the freezing temperature displays three regimes as a function of the diameter of the graphitic disks: i) Graphitic surfaces with diameter D = 4 nm freeze water at the same temperature as the larger periodic graphite surface. ii) Lamellae of diameter 2.5 nm promote heterogeneous nucleation of ice (see also Figure 6) but with about half the freezing efficiency ΔT_f of the 5 × 5 nm^2 periodic graphite surfaces and the 4 nm diameter disk. iii) Nucleation of ice in the presence of graphitic lamellae of diameters 2.25 nm and smaller proceeds mostly through a homogeneous mechanism. An exception to the latter was observed in one of the simulations with the 2.15 nm disk, for which ice nucleated at the graphitic surface at 208 K. We note that the crossover between heterogeneous and homogeneous nucleation occurs for lamellae with diameters comparable to the dimensions of the critical ice nucleus, about 2 nm. When the size of the surface is smaller than the size of the critical nucleus for heterogeneous nucleation, the contribution of the surface to the stabilization of the crystallite is negligible, and thus a higher level of undercooling is needed to overcome the free energy barrier for nucleation. Interestingly, fluctuating patches of hexagonal bilayer water form even on the surface of lamellae that are too small to be effective for heterogeneous ice nucleation: these ordered patches are too small to sustain the creation of a critical crystallite.

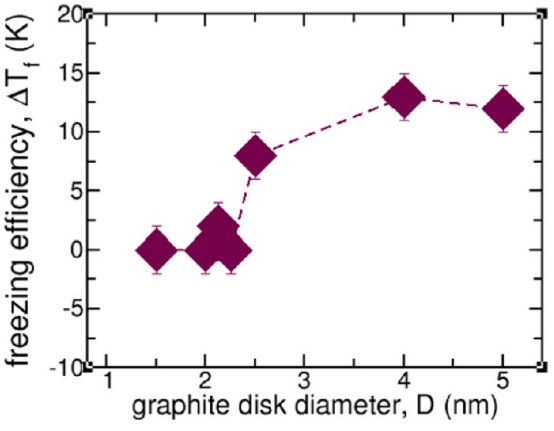

Figure 5. Freezing efficiency of the graphitic lamellae decreases as their diameter decreases below 4 nm. Graphitic disk diameters ranges from 1.5 to 4 nm, and the freezing point at 5 nm corresponds to the value for the "infinite" graphite surface of 5 nm lateral dimension. For each system 5 independent simulations have been performed at the 1 K/ns cooling rate; the size of the symbols corresponds to the error bars.

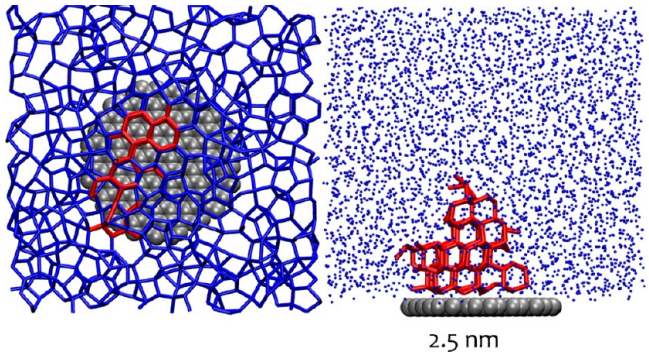

Figure 6. Heterogeneous nucleation of ice on a graphitic lamella. Snapshot of the simulation box during crystallization of water in contact with the graphitic disk of 2.5 nm of diameter. Interfacial water molecules at the edges of the lamellae display less ice-like order than around the center. A lateral view is shown on the right panel, and the correspondent front view on the left. In the front view only the first two layers of water at the surface are shown. Graphite is shown with gray balls, liquid water with blue dots, and the largest ice cluster with red sticks. In the left panel liquid water is shown with blue sticks to highlight the presence of bilayer hexagonal patches in correspondence with the graphitic disk.

The radius of curvature R_C of the lamellae in soot ranges from 2 to 50 nm.[22] We evaluated the freezing temperatures of bulk water (10,000 molecules) in contact with 5 × 5 nm^2 graphitic surfaces with R_C ranging from infinite (i.e., planar surface) to 2 nm. The curvature of the lamellae lowered its effectiveness in nucleating ice (Table 1). The surface with R_C =

Table 1. Effect of Radius of Curvature R_C on the Freezing Efficiency ΔT_f

R_C (nm)	ΔT_f (K)
infinite	13 ± 2
27.1	9 ± 2
6.8	7 ± 2
2.0	0 ± 1

dx.doi.org/10.1021/ja411507a | J. Am. Chem. Soc. 2014, 136, 3156−3164

27.1 nm produced heterogeneous freezing at a temperature very close to the one of the planar surface. Heterogeneous nucleation was never observed for the most curved lamellae, R_C = 2 nm. Also, the presence of the lamellae with R_C = 2 nm hindered the growth of the ice crystals homogeneously nucleated in the simulation cell. Liquid water presents pronounced layering at the surface (Figure 7, panel A) for all

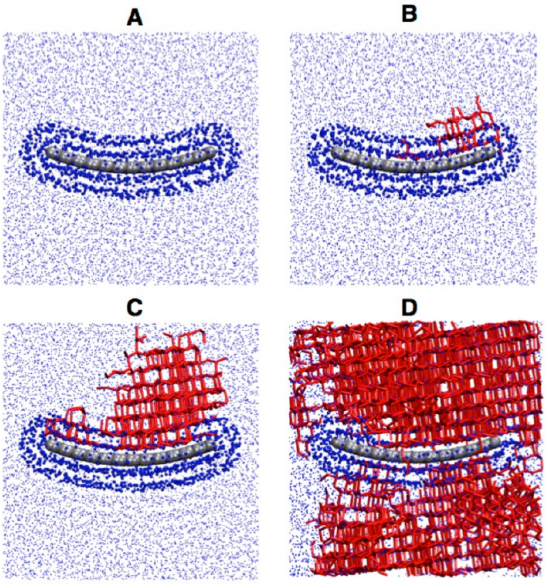

Figure 7. Isothermal crystallization of water in the presence of a curved graphitic surface. The graphitic surface has a radius of curvature R_C = 6.8 nm and is immersed in a periodic simulation cell with 10,000 water molecules. The temperature of the system was 210 K. The graphitic surface is shown with gray balls, liquid water with blue dots, and the largest ice cluster with red sticks. Blue balls are used to highlight the first two layers of water at the surface, irrespective of whether they are crystalline or liquid.

the radii of curvature, even for R_C = 2 nm that does not promote heterogeneous nucleation of ice. Fluctuating patches of bilayer hexagons on both convex and concave surfaces occurred for lamellae with radius of curvature 27.1 and 6.8 nm but not for graphitic surface with R_C = 2 nm for which interfacial water shows an abundance of five-member rings. The same as for the atomically rough surface in section A, we find an absence of ice-like order of water at surfaces that do not promote heterogeneous nucleation of ice.

Our results demonstrate that variations in soot nanostructure within the ranges reported in experiments are able to account for the observed dispersion in ice freezing temperatures.[2,18,20] The heterogeneous crystallization of water in the presence of curved graphitic lamellae proceeds on both the concave and convex surfaces. The convex surface would be representative of the one exposed by graphitic particles in soot. While in the case of hard sphere particles[121] it has been observed preferential crystallization at the convex surface, in our simulations the formation of the critical nuclei is observed with similar probability on the two sides of the graphitic surface. This indicates that the free energy barriers for the heterogeneous nucleation are comparable on the two sides of the surfaces.

When nucleation happens at a curved surface the dilemma of water is to either pay the energetic cost to bend the crystal to conform it to the surface or to pay the price to melt the surface of the crystallite in contact with the curved surface. If the radius of curvature is comparable to the size of the critical ice nucleus, then the stabilization of the nucleus by the surface is expected to be small compared to the energy cost of conforming the crystal to the curved surface, hindering the heterogeneous nucleation at the curved surface. That scenario has been reported for hard spheres,[121−123] a colloidal suspension,[124] and in theoretical calculations.[125−128] Previous studies indicate that the nucleation of ice in highly curved and atomically rough, silica-like, or hydrophobic nanopores is homogeneous,[65,129] and a premelted layer of water occurs between the ice and the surface.[65,86,87,129−133] Ice crystallization within narrow carbon nanotubes, with less than a 2 nm diameter, results in the formation of polymorphs different from ice I and with structures that depend on the pore size, which conform to the surface and do not display a premelted layer.[82,134,135] We find that water crystallization on the graphitic lamellae with radius of curvature 27.1 and 6.8 nm does not result in the formation of a premelted layer between the critical crystallite and the surface. The critical nucleus conforms to the curved surface (panel B of Figure 7), although a significant amount of defects and disordered water molecules are noticeable at the interface between the grown crystallite and the graphitic surface (panel D of Figure 7). We conclude that for graphitic surfaces with radius of curvature larger than the size of the critical nucleus melting the surface of critical crystal at the surface is more expensive than bending it.

CONCLUSIONS

We studied the heterogeneous nucleation of ice from liquid water in contact with carbon surfaces using molecular dynamics simulations. The graphitic surfaces of this study span the range of lamellae sizes and radii of curvature reported in experimental characterizations of soot. The use of the efficient coarse-grained model of water mW allowed for the study of large systems not affected by finite size effects and at least five repetitions of the calculation of the freezing temperatures for each of the surfaces. In agreement with the experiments, the simulations indicate that graphitic surfaces promote the heterogeneous nucleation of ice. Planar graphite lamellae with diameter $D \geq 4$ nm produce the highest increase in freezing temperature: 12 ± 3 K above the homogeneous nucleation temperature. The experimental maximum freezing temperature for ice on carbon surfaces is 16 K above the homogeneous nucleation temperature; this maximum increase of freezing temperature may be attributed to planar extended graphite surfaces.

The atomic flatness of the surface is a relevant parameter in the heterogeneous nucleation of ice. We find that planar but molecularly rough surfaces, either with the hydrophobicity of graphite (this work) or hydrophilic (ref 56), do not promote heterogeneous nucleation of ice. The molecularly rough surface does not promote layering of liquid water or the formation of fluctuating patches of hexagonal bilayer ice at the interface observed for graphite. The results here presented for carbon, together with the results for kaolinite[35] and AgI[70] strongly suggest that ordering of interfacial liquid water may play a role in the mechanism of heterogeneous nucleation of ice. Whether this is true for any surface, and what is the actual role played by the ordering of interfacial water in the mechanism of ice nucleation, are important questions that will be addressed in future studies.

The decreased size of lamellae lowers the effectiveness of graphitic surfaces in nucleating ice. The size of the critical nucleus (100 to 200 molecules, about 2 nm diameter)

dx.doi.org/10.1021/ja411507a | J. Am. Chem. Soc. 2014, 136, 3156−3164

determines the crossover from the heterogeneous to homogeneous ice nucleation mechanism. The free energy of stabilization of the critical nucleus by the surface decreases sharply when the dimensions of the nucleus and the surface are comparable, resulting in a higher level of supercooling needed to stabilize a critical nucleus. Lamellae with diameter 2.5 nm have a nucleation efficiency $\Delta T_f = T_f - T_f^{homo}$ that is is 50% of the one for the extended graphite surface. It is important to note that the crossover occurs within the range of dimensions that are relevant for soot. The ice nucleating efficiency of soot lamellae also decreases with the decrease in their radii of curvature because the curved surface increases the free energy of the crystalline nucleus. Nucleation of ice is heterogeneous for graphitic surfaces with radius of curvature down to at least 6.8 nm and already homogeneous when R_C = 2 nm. The crossover from heterogeneous to homogeneous freezing temperatures is, again, within the range of curvatures observed for soot. We conclude that the dispersion in the size and radius of curvature of the lamellae alone could account for the wide range of the experimental freezing temperatures reported for soot.[2,18,20]

The sensitivity of the ice freezing temperatures to the dimensions of the graphitic surfaces calls for a nanostructural characterization of soot. Changes in the chemistry of the surface may also affect soot's ability to promote nucleation of ice.[39−43] In separate work, we found that hydroxylation of graphitic surfaces *decreases* their ice nucleation efficiency.[56] It should be noted that templating by the surface is not involved in the heterogeneous nucleation of ice on bare and uniformly hydroxylated model graphitic surfaces. As the spatial distribution of functional groups in soot is not yet known, uniform distributions of hydroxyl groups were considered in ref 56. An experimental characterization of the amount and distribution of functional groups on soot is needed to further the understanding of their impact in the mechanisms and temperature of crystallization of ice. Statistical models that integrate the experimental characterization of soot nanostructure and spatial distribution of functional groups, with the results of the simulations on model graphitic systems, may be built to predict the ice freezing temperatures in complex soot particles.

The critical ice nuclei for heterogeneous nucleation on graphite and for homogeneous nucleation[59] have comparable sizes. The freezing temperatures T_f were determined in the two cases at the same cooling rate; therefore, the crystallization rates at these distinct T_f should also be similar. Within the framework of classical nucleation theory (CNT), the nucleation rate is a product of a pre-exponential term that depends on the rate of attachment of new monomers to the ice surface and a term that decreases exponentially with the nucleation barrier, $exp(-\Delta G^{\#}/RT)$.[136] If the pre-exponential factor does not have a steep dependence on temperature, then comparable crystallization rates for homogeneous and heterogeneous nucleation would imply that the free energy barriers for the two processes are essentially the same. As the size of the nucleation barrier determines the size of the critical crystallite that can successfully grow ice, this may be the explanation for our finding of similar sizes of critical nuclei for homogeneous and heterogeneous nucleation measured at the same crystallization rate. Based on these results, we conjecture that the size of the ice critical nucleus depends mostly on the crystallization rate and not so much on the freezing temperature if the rates are fixed. This would have important consequences for the quest of the active nucleating sites in complex particles, such as bacteria or aerosols, which can have overall dimensions above micrometers. The active nucleating surfaces of these large particles may have dimensions as small as a few nanometers, posing significant challenges for their finding and characterization in experiments.

AUTHOR INFORMATION

Corresponding Author

Valeria.Molinero@utah.edu

Notes

The authors declare no competing financial interest.

ACKNOWLEDGMENTS

This work was supported by the National Science Foundation through awards CHE-1125235 and CHE-1309601. We thank the Center for High performance Computing at the University of Utah for technical support and allocation of computer time.

REFERENCES

(1) Baker, M. B.; Peter, T. *Nature* **2008**, *451*, 299.
(2) Murray, B. J.; O'Sullivan, D.; Atkinson, J. D.; Webb, M. E. *Chem. Soc. Rev.* **2012**, *41*, 6519.
(3) Hoose, C.; Möhler, O. *Atmos. Chem. Phys.* **2012**, *12*, 9817.
(4) Hoose, C.; Kristjánsson, J. E.; Chen, J. P.; Hazra, A. *J. Atmos. Sci.* **2010**, *67*, 2483.
(5) Moreno, L. L.; Stetzer, O.; Lohmann, U. *Atmos. Chem. Phys.* **2013**, *13*, 9745.
(6) Atkinson, J. D.; Murray, B. J.; Woodhouse, M. T.; Whale, T. F.; Baustian, K. J.; Carslaw, K. S.; Dobbie, S.; O' Sullivan, D.; Malkin, T. L. *Nature* **2013**, *498*, 355.
(7) Broadley, S. L.; Murray, B. J.; Herbert, R. J.; Atkinson, J. D.; Dobbie, S.; Malkin, T. L.; Condliffe, E.; Neve, L. *Atmos. Chem. Phys.* **2012**, *12*, 287.
(8) Murray, B. J.; Broadley, S. L.; Wilson, T. W.; Atkinson, J. D.; Wills, R. H. *Atmos. Chem. Phys.* **2011**, *11*, 4191.
(9) Lüönd, F.; Stetzer, O.; Welti, A. *J. Geophys. Res.* **2010**, *115*, D14201 DOI: 10.1029/2009JD012959.
(10) Pinti, V.; Marcolli, C.; Zobrist, B.; Hoyle, C. R.; Peter, T. *Atmos. Chem. Phys.* **2012**, *12*, 5859.
(11) Koop, T.; Zobrist, B. *Phys. Chem. Chem. Phys.* **2009**, *11*, 10839.
(12) Zobrist, B.; Marcolli, C.; Peter, T.; Koop, T. *J. Phys. Chem. A* **2008**, *112*, 3965.
(13) Zobrist, B.; Koop, T.; Luo, B. P.; Marcolli, C.; Peter, T. *J. Phys. Chem. C* **2007**, *111*, 2149.
(14) Knopf, D. A.; Koop, T. *J. Geophys. Res.* **2006**, *111*, D12201 DOI: 10.1029/2005JD006894.
(15) Lohmann, U.; Kärcher, B.; Hendricks, J. *J. Geophys. Res.* **2004**, *109*, D16204 DOI: 10.1029/2003JD004443.
(16) Gierens, K. *Atmos. Chem. Phys.* **2003**, *3*, 437.
(17) Twohy, C. H.; DeMott, P. J.; Pratt, K. A.; Subramanian, R.; Kok, G. L.; Murphy, S. M.; Lersch, T.; Heymsfield, A. J.; Wang, Z.; Prather, K. A.; Seinfeld, J. H. *J. Atmos. Sci.* **2010**, *67*, 2437.
(18) DeMott, P. J. *J. Appl. Meteorol.* **1990**, *29*, 1072.
(19) DeMott, P. J.; Chen, Y.; Kreidenweis, S. M.; Rogers, D. C.; Sherman, D. E. *Geophys. Res. Lett.* **1999**, *26*, 2429.
(20) Diehl, K.; Mitra, S. K. *Atmos. Environ.* **1998**, *32*, 3145.
(21) Gorbunov, B.; Baklanov, A.; Kakutkina, N.; Windsor, H. L.; Toumi, R. *J. Aerosol Sci.* **2001**, *32*, 199.
(22) Popovicheva, O.; Kireeva, E.; Persiantseva, N.; Khokhlova, T.; Shonija, N.; Tishkova, V.; Demirdjian, B. *Atmos. Res.* **2008**, *90*, 326.
(23) Möhler, O.; Linke, C.; Saathoff, H.; Schnaiter, M.; Wagner, R.; Mangold, A.; Krämer, M.; Schurath, U. *Meteorol. Z.* **2005**, *14*, 477.
(24) Möhler, O.; Büttner, S.; Linke, C. *J. Geophys. Res.* **2005**, *110*, D11210 DOI: 10.1029/2004JD005169.
(25) Dymarska, M.; Murray, B. J.; Sun, L.; Eastwood, M. L.; Knopf, D. A.; Bertram, A. K. *J. Geophys. Res.* **2006**, *111*, D04204 DOI: 10.1029/2005JD006627.

(26) Fornea, A. P.; Brooks, S. D.; Dooley, J. B.; Saha, A. *J. Geophys. Res.* **2009**, *114*, D13201 DOI: 10.1029/2009JD011958.
(27) Koehler, K. A.; DeMott, P. J.; Kreidenweis, S. M.; Popovicheva, O. B.; Petters, M. D.; Carrico, C. M.; Kireeva, E. D.; Khokhlova, T. D.; Shonija, N. K. *Phys. Chem. Chem. Phys.* **2009**, *11*, 7906.
(28) Crawford, I.; Möhler, O.; Schnaiter, M.; Saathoff, H.; Liu, D.; McMeeking, G.; Linke, C.; Flynn, M.; Bower, K. N.; Connolly, P. J.; Gallagher, M. W.; Coe, H. *Atmos. Chem. Phys.* **2011**, *11*, 9549.
(29) Kong, X.; Andersson, P. U.; Thomson, E. S.; Pettersson, J. B. C. *J. Phys. Chem. C* **2012**, *116*, 8964.
(30) Yakobi-Hancock, J. D.; Ladino, L. A.; Abbatt, J. P. D. *Atmos. Chem. Phys. Discuss.* **2013**, *13*, 17299.
(31) Kanji, Z. A.; Welti, A.; Chou, C.; Stetzer, O.; Lohmann, U. *Atmos. Chem. Phys.* **2013**, *13*, 9097.
(32) Zhang, J.; Jin, D.; Zhao, L.; Liu, X.; Lian, J.; Li, G.; Jiang, Z. *Adv. Powder Technol.* **2011**, *22*, 613.
(33) Pruppacher, H. R.; Klett, J. D. *Microphysics of Clouds and Precipitation*; Kluwer: Dordrecht, 1997.
(34) Popovitz-Biro, R.; Wang, J. L.; Majewski, J.; Shavit, E.; Leiserowitz, L.; Labav, M. *J. Am. Chem. Soc.* **1994**, *116*, 1179.
(35) Cox, S. J.; Raza, Z.; Kathmann, S.; Slater, B.; Michaelides, A. *Faraday Discuss.* **2013**, DOI: 10.1039/C3FD00059A.
(36) Penner, J. E.; Eddleman, H.; Novakov, T. *Atmos. Environ., Part A* **1993**, *27 A*, 1277.
(37) Lary, D. J.; Shallcross, D. E.; Toumi, R. *J. Geophys. Res.* **1999**, *104*, 15929.
(38) Hudson, P. K.; Murphy, D. M.; Cziczo, D. J.; Thomson, D. S.; de Gouw, J. A.; Warneke, C.; Holloway, J.; Jost, H. J.; Hübler, G. *J. Geophys. Res.* **2004**, *109*, D23S27 DOI: 10.1029/2003JD004398.
(39) Friedman, B.; Kulkarni, G.; Beránek, J.; Zelenyuk, A.; Thornton, J. A.; Cziczo, D. J. *J. Geophys. Res.* **2011**, *116*, D17203 DOI: 10.1029/2011JD015999.
(40) Knopf, D. A.; Wang, B.; Laskin, A.; Moffet, R. C.; Gilles, M. K. *Geophys. Res. Lett.* **2010**, *37*, L11803 DOI: 10.1029/2010GL043362.
(41) Wang, B.; Knopf, D. A. *J. Geophys. Res., D: Atmos.* **2011**, *116*, D03205 DOI: 10.1029/2010JD014964.
(42) Zuberi, B. *Geophys. Res. Lett.* **2005**, *32*, L01807 DOI: 10.1029/2004GL021496.
(43) Schill, G. P.; Tolbert, M. A. *J. Phys. Chem. A* **2012**, *116*, 6817.
(44) Cabrera-Sanfelix, P.; Darling, G. R. *J. Phys. Chem. C* **2007**, *111*, 18258.
(45) Oubal, M.; Picaud, S.; Rayez, M. T.; Rayez, J. C. *Carbon* **2010**, *48*, 1570.
(46) Yan, J. A.; Xian, L.; Chou, M. Y. *Phys. Rev. Lett.* **2009**, 103.
(47) Vander Wal, R. L.; Strzelec, A.; Toops, T. J.; Daw, C. S. In *Spring Technical Meetingof the Central States Section of the Combustion Institute*; Oak Ridge National Laboratory (ORNL); Fuels, Engines and Emissions Research Center: 2012; Vol. April 22−24, 2012.
(48) Popovicheva, O. B.; Persiantseva, N. M.; Kuznetsov, B. V.; Rakhmanova, T. A.; Shonija, N. K.; Suzanne, J.; Ferry, D. *J. Phys. Chem. A* **2003**, *107*, 10046.
(49) Vander Wal, R. L.; Bryg, V. M.; Hays, M. D. *Anal. Chem.* **2011**, *83*, 1924.
(50) Han, C.; Liu, Y.; Liu, C.; Ma, J.; He, H. *J. Phys. Chem. A* **2012**, *116*, 4129.
(51) Casabianca, L. B.; Shaibat, M. A.; Cai, W. W.; Park, S.; Piner, R.; Ruoff, R. S.; Ishii, Y. *J. Am. Chem. Soc.* **2010**, *132*, 5672.
(52) Cai, W.; Piner, R. D.; Stadermann, F. J.; Park, S.; Shaibat, M. A.; Ishii, Y.; Yang, D.; Velamakanni, A.; Sung, J. A.; Stoller, M.; An, J.; Chen, D.; Ruoff, R. S. *Science New Series* **2008**, *321*, 1815.
(53) Vander Wal, R. L.; Bryg, V. M.; Hays, M. D. *J. Aerosol Sci.* **2009**, *41*, 108.
(54) Vander Wal, R. L.; Tomasek, A. J. *Combust. Flame* **2004**, *136*, 129.
(55) Pósfai, M.; Simonics, R.; Li, J.; Hobbs, P. V. *J. Geophys. Res.* **2003**, *108*, 8483.
(56) Lupi, L.; Molinero, V. *J. Phys. Chem. A* **2013**, under review.
(57) Svishchev, I.; Kusalik, P. *Phys. Rev. Lett.* **1994**, *73*, 975.
(58) Li, T.; Donadio, D.; Russo, G.; Galli, G. *Phys. Chem. Chem. Phys.* **2011**, *13*, 19807.
(59) Moore, E. B.; Molinero, V. *Nature* **2011**, *479*, 506.
(60) Matsumoto, M.; Saito, S.; Ohmine, I. *Nature* **2002**, *416*, 409.
(61) Reinhardt, A.; Doye, J. P. K. *J. Chem. Phys.* **2012**, *136*, 054501.
(62) Reinhardt, A.; Doye, J.; Noya, E. G.; Vega, C. *J. Chem. Phys.* **2012**, *137*, 194504.
(63) Bullock, G.; Molinero, V. *Faraday Discuss.* **2013**, DOI: 10.1039/C3FD00085K.
(64) Johnston, J. C.; Molinero, V. *J. Am. Chem. Soc.* **2012**, *134*, 6650.
(65) Moore, E. B.; de la Llave, E.; Welke, K.; Scherlis, D. A.; Molinero, V. *Phys. Chem. Chem. Phys.* **2010**, *12*, 4124.
(66) Li, T.; Donadio, D.; Galli, G. *Nat. Commun.* **2013**, *4*, doi:10.1038/ncomms2918.
(67) Sanz, E.; Vega, C.; Espinosa, J. R.; Caballero-Bernal, R.; Abascal, J. L. F.; Valeriani, C. *J. Am. Chem. Soc.* **2013**, *135*, 15008.
(68) Picaud, S.; Collignon, B.; Hoang, P. N. M.; Rayez, J. C. *J. Phys. Chem. B* **2006**, *110*, 8398.
(69) Picaud, S.; Collignon, B.; Hoang, P. N. M.; Rayez, J.-C. *PCCP: Phys. Chem. Chem. Phys.* **2008**, *10*, 6998.
(70) Taylor, J.; Hale, B. *Phys. Rev. B* **1993**, *47*, 9732.
(71) Fang, J. X.; Marlow, W. H.; Lu, J. X.; Lucchese, R. R. *J. Chem. Phys.* **1997**, *107*, 5212.
(72) Croteau, T.; Bertram, A. K.; Patey, G. N. *J. Phys. Chem. A* **2008**, *112*, 10708.
(73) Croteau, T.; Bertram, A. K.; Patey, G. N. *J. Phys. Chem. A* **2009**, *113*, 7826.
(74) Moulin, F.; Picaud, S.; Hoang, P. N. M.; Jedlovszky, P. *J. Chem. Phys.* **2007**, *127*, 164719.
(75) Hantal, G.; Picaud, S.; Hoang, P. N. M.; Voloshin, V. P.; Medvedev, N. N.; Jedlovszky, P. *J. Chem. Phys.* **2010**, *133*, 144702 1.
(76) Hu, X. L.; Michaelides, A. *Surf. Sci.* **2008**, *602*, 960.
(77) Hu, X. L.; Michaelides, A. *Surf. Sci.* **2007**, *601*, 5378.
(78) Yan, J. Y.; Patey, G. N. *J. Chem. Phys* **2013**, *139*, 144501.
(79) Yan, J. Y.; Patey, G. N. *J. Phys. Chem.. A* **2012**, *116*, 7057.
(80) Yan, J. Y.; Patey, G. N. *J. Phys. Chem. Lett.* **2011**, *2*, 2555.
(81) Koga, K.; Gao, G.; Tanaka, H.; Zeng, X. *Nature* **2001**, *412*, 802.
(82) Shiomi, J.; Kimura, T.; Maruyama, S. *J. Phys. Chem. C* **2007**, *111*, 12188.
(83) Kastelowitz, N.; Johnston, J. C.; Molinero, V. *J. Chem. Phys.* **2010**, *132*, 124511.
(84) Molinero, V.; Moore, E. B. *J. Phys. Chem. B* **2009**, *113*, 4008.
(85) Moore, E. B.; Molinero, V. *J. Chem. Phys.* **2009**, *130*, 244505.
(86) Moore, E. B.; Allen, J. T.; Molinero, V. *J. Phys. Chem. C* **2012**, *116*, 7507.
(87) Limmer, D. T.; Chandler, D. *J. Chem. Phys.* **2012**, *137*, 044509.
(88) Limmer, D. T.; Chandler, D. *J. Chem. Phys.* **2011**, *135*, 134503.
(89) Holten, V.; Limmer, D. T.; Molinero, V.; Anisimov, M. A. *J. Chem. Phys.* **2013**, *138*, 174501 1.
(90) Shadrack Jabes, B.; Nayar, D.; Dhabal, D.; Molinero, V.; Chakravarty, C. *J. Phys.: Condens. Matter* **2012**, *24*, 284116.
(91) Hujo, W.; Jabes, B. S.; Rana, V. K.; Chakravarty, C.; Molinero, V. *J. Stat. Phys.* **2011**, *145*, 293.
(92) Moore, E. B.; Molinero, V. *Phys. Chem. Chem. Phys.* **2011**, *13*, 20008.
(93) Moore, E. B.; Molinero, V. *J. Chem. Phys.* **2010**, *132*, 244504.
(94) Humphrey, W.; Dalke, A.; Schulten, K. *J. Mol. Graphics* **1996**, *14*, 33.
(95) Stillinger, F. H.; Weber, T. A. *Phys. Rev. B* **1985**, *31*, 5262.
(96) Adamson, A. W.; Gast, A. P. *Wiley Interscience Publication, Physical Chemistry of Surfaces*; John Wiley & Sons, Inc.: New York, 1997.
(97) Li, H.; Zeng, X. C. *ACS Nano* **2012**, *6*, 2401.
(98) Plimpton, S. J. *J. Comput. Phys.* **1995**, *117*, 1.
(99) Steinhardt, P. J.; Nelson, D. R.; Ronchetti, M. *Phys. Rev. B: Condens. Matter Mater. Phys.* **1983**, *28*, 784.
(100) Malkin, T. L.; Murray, B. J.; Brukhno, A. V.; Anwar, J.; Salzmann, C. G. *Proc. Natl. Acad. Sci.* **2012**, *109*, 1041.

(101) Hansen, T.; Koza, M.; Kuhs, W. *J. Phys.: Condens. Matter* **2008**, *20*, 285104.
(102) Kuhs, W. F.; Sippel, C.; Falenty, A.; Hansen, T. C. *Proc. Natl. Acad. Sci.* **2012**, *109*, 21259.
(103) Yang, D. S.; Zewail, A. H. *Proc. Natl. Acad. Sci. U.S.A.* **2009**, *106*, 4122.
(104) Liu, J.; Nicholson, C. E.; Cooper, S. J. *Langmuir* **2007**, *23*, 7286.
(105) Cicero, G.; Grossman, J. C.; Schwegler, E.; Gygi, F.; Galli, G. *J. Am. Chem. Soc.* **2008**, *130*, 1871.
(106) Argyris, D.; Tummala, N. R.; Striolo, A.; Cole, D. R. *J. Phys. Chem. C* **2008**, *112*, 13587.
(107) Zettlemoyer, A. C.; Tcheurekdjian, N.; Chessick, J. J. *Nature* **1961**, *192*, 653.
(108) Finnegan, W. G.; Chai, S. K. *J. Atmos. Sci.* **2003**, *60*, 1723.
(109) Gavish, M.; Popovitz-Biro, R.; Lahav, M.; Leiserowitz, L. *Science* **1990**, *250*, 973.
(110) Kawasaki, T.; Tanaka, H. *Proc. Natl. Acad. Sci. U.S.A.* **2010**, *107*, 14036.
(111) Jacobson, L. C.; Hujo, W.; Molinero, V. *J. Am. Chem. Soc.* **2010**, *132*, 11806.
(112) Jacobson, L. C.; Hujo, W.; Molinero, V. *J. Phys. Chem. B* **2010**, *114*, 13796.
(113) Vatamanu, J.; Kusalik, P. G. *Phys. Chem. Chem. Phys.* **2010**, *12*, 15065.
(114) Kawasaki, T.; Tanaka, H. *J. Phys.: Condensed Matter* **2010**, *22*, 232102.
(115) Raiteri, P.; Gale, J. D. *J. Am. Chem. Soc.* **2010**, *132*, 17623.
(116) Ten Wolde, P. R.; Frenkel, D. *Science* **1997**, *277*, 1975.
(117) Lutsko, J. F. *J. Chem. Phys.* **2012**, *136*, 034509.
(118) Russo, J.; Tanaka, H. *Sci. Rep.* **2012**, *2*, DOI: 10.1038/srep00505.
(119) Leocmach, M.; Tanaka, H. *Nat. Commun.* **2012**, *3*, DOI: 10.1038/ncomms1974.
(120) Vander Wal, R. L.; Bryg, V. M.; Hays, M. D. *J. Aerosol Sci.* **2010**, *41*, 108.
(121) Cacciuto, A.; Auer, S.; Frenkel, D. *Nature* **2004**, *428*, 404.
(122) Bryk, P.; Roth, R.; Mecke, K.; Dietrich, S. *Phys. Rev. E* **2003**, *68*, 031602 1.
(123) Laird, B. B.; Hunter, A.; Davidchack, R. L. *Phys. Rev. E: Stat., Nonlinear, Soft Matter Phys.* **2012**, *86*, 060602 1.
(124) Ziese, F.; Maret, G.; Gasser, U. *J. Phys.: Condens. Matter* **2013**, *25*, 375105.
(125) Fletcher, N. H. *J. Chem. Phys.* **1958**, *29*, 572.
(126) Qian, M. *Acta Mater.* **2007**, *55*, 943.
(127) Qian, M.; Ma, J. *J. Chem. Phys.* **2009**, *130*, 214709.
(128) Cooper, S. J.; Nicholson, C. E.; Liu, J. *J. Chem. Phys.* **2008**, *129*, 124715 1.
(129) González Solveyra, E.; De La Llave, E.; Scherlis, D. A.; Molinero, V. *J. Phys. Chem. B* **2011**, *115*, 14196.
(130) Schreiber, A.; Ketelsen, I.; Findenegg, G. H. *PCCP: Phys. Chem. Chem. Phys.* **2001**, *3*, 1185.
(131) Jaehnert, S.; Chavez, F. V.; Schaumann, G. E.; Schreiber, A.; Schoenhoff, M.; Findenegg, G. H. *PCCP: Phys. Chem. Chem. Phys.* **2008**, *10*, 6039.
(132) Jelassi, J.; Castricum, H.; Bellissent-Funel, M.-C.; Dore, J.; Webber, J.; Sridi-Dorbez, R. *PCCP: Phys. Chem. Chem. Phys.* **2010**, *12*, 2838.
(133) Deschamps, J.; Audonnet, F.; Brodie-Linder, N.; Schoeffel, M.; Alba-Simionesco, C. *PCCP: Phys. Chem. Chem. Phys.* **2010**, *12*, 1440.
(134) Koga, K.; Gao, G. T.; Tanaka, H.; Zeng, X. C. *Nature* **2001**, *412*, 802.
(135) Maniwa, Y.; Kataura, H.; Abe, M.; Udaka, A.; Suzuki, S.; Achiba, Y.; Kira, H.; Matsuda, K.; Kadowaki, H.; Okabe, Y. *Chem. Phys. Lett.* **2005**, *401*, 534.
(136) Kashchiev, D. *Nucleation. Basic theory and applications*; Butterworth Heinemann: Oxford, 2000.